JOURNAL OF THE ROYAL SOCIETY Interface

The adhesion model considering capillarity for gecko attachment system

Tae Wan Kim and Bharat Bhushan

J. R. Soc. Interface 2008 **5**, 319-327
doi: 10.1098/rsif.2007.1078

JOURNAL OF THE ROYAL SOCIETY Interface

J. R. Soc. Interface (2008) **5**, 319–327
doi:10.1098/rsif.2007.1078
Published online 26 June 2007

The adhesion model considering capillarity for gecko attachment system

Tae Wan Kim and Bharat Bhushan*

Nanotribology Laboratory for Information Storage and MEMS/NEMS, The Ohio State University, 201 West 19th Avenue, Columbus, OH 43210-1142, USA

Geckos make use of approximately a million microscale hairs (setae) that branch off into hundreds of nanoscale spatulae to cling to different smooth and rough surfaces and detach at will. This hierarchical surface construction gives the gecko the adaptability to create a large real area of contact with surfaces. It is known that van der Waals force is the primary mechanism used to adhere to surfaces, and capillary force is a secondary effect that can further increase adhesive force. To investigate the effects of capillarity on gecko adhesion, we considered the capillary force as well as the solid-to-solid interaction. The capillary force expressed in terms of elliptical integral is calculated by numerical method to cope with surfaces with a wide range of contact angles. The adhesion forces exerted by a single gecko spatula in contact with planes with different contact angles for various relative humidities are calculated, and the contributions of capillary force to total adhesion force are evaluated. The simulation results are compared with experimental data. Finally, using the three-level hierarchical model recently developed to simulate a gecko seta contacting with random rough surface, the effect of the relative humidity and the hydrophobicity of surface on the gecko adhesion is investigated.

Keywords: gecko; capillarity; adhesion; hierarchical structure

1. INTRODUCTION

Several creatures including insects, spiders and lizards have a unique ability to cling to and detach from ceilings and walls using their attachment systems. Although the foot morphology of these animals is different, in most cases there are small hairs that cover the surfaces of the pads of their feet, called setae. Using setae, animals develop intimate contact with a substrate that provides enough attachment force to cling to and crawl on a wide range of natural and artificial surfaces and have reversible adhesion properties. They retain the ability to remove their feet from the attachment surface at will by peeling action. This universal attachment and detachment ability of animals is referred to as 'smart adhesion' (Bhushan *et al.* 2006), which is of both scientific and practical interests.

The most advanced attachment ability in lizards is found in the *Tokay gecko* or *Gekko gecko* (Hiller 1968; Irschick *et al.* 1996). Measurement of the adhesion force of a single seta was carried out by Autumn *et al.* (2000). The attachment pads of a *T. gecko* have total area of two feet of the order of 200 mm^2, which can produce a clinging ability of approximately 20 N (vertical force required to pull a lizard down from a nearly vertical (85°) surface; Irschick *et al.* 1996). In isolated gecko setae, a 2.5 μN preload yielded adhesion of 20–40 μN (Autumn *et al.* 2002) and thus an adhesion coefficient, which represents the strength of adhesion with respect to preload, of 8–16.

With regard to the natural living conditions of the animals, we can separate the mechanics of gecko attachment into two parts: the mechanics of adhesion of a single contact with a flat surface and an adaptation of a large number of spatulae to a natural rough surface. Modelling of the mechanics of adhesion of spatulae to a smooth surface was developed by Autumn *et al.* (2002), Jagota & Bennison (2002) and Arzt *et al.* (2003). In the model by Arzt *et al.* (2003), the adhesion force was calculated using a thermodynamical surface energy approach. The authors assumed that a spatula was a hemisphere with radius R. For the calculation of adhesion force F_{ad}, the JKR approach was used (Johnson *et al.* 1971; Bhushan 1999, 2003) with $F_{ad} = -(3/2)\pi R E_{ad}$, where E_{ad} is the work of adhesion per unit area. It can be seen that the adhesion force of multiple contacts F'_{ad} can be increased by dividing the contact into a large number (N_c) of small contacts, while the nominal area of the contact remains the same, $F'_{ad} \sim \sqrt{N_c}$. However, this model only considers contact with a flat surface. On natural rough surfaces, the compliance and adaptability of setae are the primary sources of high adhesion. Intuitively, the hierarchical structure of gecko setae allows for a greater contact with a natural rough surface than a non-branched attachment system (Sitti & Fearing 2003). In the design of fibrillar structures, it is necessary to ensure

*Author for correspondence (bhushan.2@osu.edu).

Received 17 April 2007
Accepted 30 May 2007

that the fibrils are compliant enough to easily deform to the mating surface's roughness profile, yet rigid enough not to collapse under their own weight. Spacing of the individual fibrils is also important. If the spacing is too small, adjacent fibrils can attract each other through intermolecular forces which will lead to bunching. In order to overcome these problems, a multi-level compliant system is being studied (Sitti 2003; Northen & Turner 2005). Recently, Bhushan *et al.* (2006) and Kim & Bhushan (2007) developed two- and three-level hierarchical models using the spring structure contacting with a random rough surface and showed the effect of hierarchical structure on adhesion enhancement. Kim & Bhushan (in press) showed the effect of stiffness of multi-level hierarchical attachment system on adhesion enhancement.

The majority of experimental results point towards van der Waals forces as the dominant mechanism of adhesion (Autumn *et al.* 2000; Bergmann & Irschick 2005). Recent research suggests that capillary forces can be a contributing adhesive factor (Huber *et al.* 2005). Capillary forces created by humidity naturally present in the air can further increase the adhesive force generated by the spatulae. Orr *et al.* (1975) formulated the mean curvature of meniscus between sphere and plane in terms of elliptical integrals which is difficult to handle. Therefore, the approximated equation is used commonly in nano applications, i.e. AFM (Stifter *et al.* 2000; Bhushan 2003). Fortes (1982) and Carter (1988) reported an analytical calculation of the force–distance relationship of a liquid bridge between two solid parallel plates with arbitrary equal contact angles at both surfaces.

In this study, we investigate the effects of the capillarity on gecko adhesion. We consider the capillary force consisting of the Laplace force and the surface tension force as well as the DMT adhesion force. The capillary force expressed in terms of an elliptical integral is calculated by numerical method to cope with surfaces with wide range of contact angles. The adhesion forces exerted by a single gecko spatula in contact with planes with different contact angles for various relative humidity are calculated and compared with experimental data in the literature (Huber *et al.* 2005). Next, we performed the adhesion analysis for three-level hierarchical model for gecko seta using contact with rough surfaces with different values of root mean square (RMS) amplitude σ.

2. ANALYSIS

Gecko adhesion is caused by the capillary force consisting of Laplace force and the surface tension, as well as the solid-to-solid interaction. The capillary force depends on both the relative humidity and the hydrophobicity (contact angle) of both spatula and mating surface. For the single spatula contact, the capillary force expressed in terms of elliptical integral is calculated by numerical method, and the DMT adhesion force is also calculated.

The simulation of seta models in contact with random rough surfaces is carried out numerically. Hierarchical morphology of gecko setae is modelled as three-level elastic springs. The spring model is pressed against the rough surface, and the elastic force arising in the springs is calculated. During pull-off, the spring force changes to a negative value after some pull-off, due to adhesion. The elastic force and the adhesion force of individual spatulae contacts are calculated. When the elastic force is less than the adhesion force, individual contact breaks and the total number of contacts at a given time is calculated. Total elastic force of the springs still in contact as a function of spring position is calculated. From the spring force–distance curves, we can extract the adhesion force F_{ad}.

In this section, first, the adhesion forces of a single contact including the capillary force and the solid-to-solid interaction by DMT theory are presented. Next, we discuss the hierarchical morphology of gecko setae and its simplification for the simulation as a three-level spring model. Typical values used in the model are presented. Then, the numerical method for calculating the adhesion force for three-level hierarchical spring model in contact with rough surfaces is presented.

2.1. Adhesion force for single spatula contact

The tip of the spatula in a single contact is assumed as spherical. Total adhesion force between a spherical tip and a plane consists of the capillary force and the solid-to-solid interaction. The capillary force F_c can be divided into two components: the Laplace force F_L and the surface tension F_s:

$$F_c = F_L + F_s. \tag{2.1}$$

The Laplace force is caused by the pressure difference across the interface of a curved liquid surface (figure 1) and depends on pressure difference$\times$meniscus area, which can be expressed as (Orr *et al.* 1975)

$$F_L = -\pi\kappa\gamma R^2 \sin^2\phi, \tag{2.2}$$

where γ is the surface tension of the liquid; R is the tip radius; ϕ is the filling angle; and κ is the mean curvature of meniscus. From the Kelvin equation (Israelachvili 1992), which is the thermal equilibrium relation, the mean curvature of meniscus can be determined as

$$\frac{\Re T}{V\gamma}\ln\left(\frac{p}{p_0}\right) = \kappa, \tag{2.3}$$

where $\Re$ is the universal gas constant; T is the absolute temperature; V is the molecular volume; p_0 is the saturated vapour pressure of the liquid at T; and p is the ambient pressure acting outside the curved surface(p/p_0 is the relative humidity).

Orr *et al.* (1975) formulated the mean curvature of meniscus between sphere and plane in terms of elliptical integrals when the contact angles on sphere and plane are different:

$$\kappa = \frac{1}{D + R(1+\cos\phi)}\{-\cos(\theta_1+\phi) - \cos\theta_2 + 2E(k_1) \pm E(\alpha_1, k_1) \pm E(\alpha_2, k_1)\} \quad \theta_2 \lesseqgtr \pi/2, \tag{2.4}$$

where D is the separation between sphere and plane; θ_1 and θ_2 are contact angles on sphere and plane,

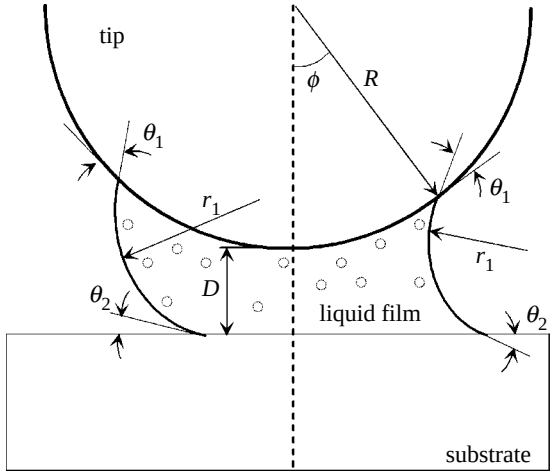

Figure 1. Schematic of a sphere on a plane at distance D with a liquid film in between, forming menisci. In this figure, R is the tip radius, ϕ is the filling angle, θ_1 and θ_2 are contact angles on sphere and plane and r_1 and r_2 are the two principal radii of the curved surface.

respectively; and E is the elliptic integral of the second kind. k_1, α_1 and α_2 are defined as (Orr *et al.* 1975)

$$k_1 = \sqrt{1+c}, \tag{2.5}$$

$$\alpha_1 = \arcsin\left(\frac{1}{k_1}\sin\left(-(\theta_1+\phi)+\frac{\pi}{2}\right)\right), \tag{2.6}$$

$$\alpha_2 = \arcsin\left(\frac{1}{k_1}\sin\left(\theta_2-\frac{\pi}{2}\right)\right), \tag{2.7}$$

where c is the curvature-dependent parameter and is defined as

$$c = \kappa^2 R^2 \sin^2\phi - 2\kappa R \sin\phi \sin(\theta_1+\phi). \tag{2.8}$$

The filling angle ϕ can be calculated from equations (2.3)–(2.8) using iteration method. Then, the Laplace force is calculated at given environment using equation (2.2).

The surface tension of the liquid results in the formation of curved liquid–air interface. The surface tension force acting on the sphere is (Orr *et al.* 1975)

$$F_s = 2\pi R\gamma \sin\phi \sin(\theta_1+\phi). \tag{2.9}$$

The surface tension force depends on radius. Therefore, division of the contacts as found in a gecko results in square root of N_c effect on the surface tension force upon division.

Hence, total capillary force on the sphere is

$$F_c = \pi R\gamma\{2\sin\phi\sin(\theta_1+\phi) - \kappa R\sin^2\phi\}. \tag{2.10}$$

For the adhesion force by the solid-to-solid interaction, two alternative models dominate the world of contact mechanics: the Johnson–Kendall–Roberts (JKR) theory (Johnson *et al.* 1971; Bhushan 1999, 2002, 2003) for compliant solids and the Derjaguin–Muller–Toporov (DMT) theory (Derjaguin *et al.* 1975; Bhushan 1999, 2002, 2003) for stiff solids. Gecko's seta is composed of β-keratin which has high elastic modulus (Russell 1986; Bertram & Gosline 1987) and is close to DMT model. Therefore, we applied the DMT theory for the solids contact. The surfaces contacting with seta are assumed to be rigid.

Assuming that both tips of a spatula and the asperity summits of the rough surface are spherical (which have a constant radius), a single spatula adhering to a rough surface can be modelled as the interaction between two spherical tips. The DMT adhesion force between two round tips is calculated as

$$F_{DMT} = 2\pi R_c E_{ad}, \tag{2.11}$$

where R_c is the reduced radius of contact, which is calculated as $R_c = (1/R_1 + 1/R_2)^{-1}$; R_1 and R_2 are radii of contacting surfaces; $R_1 = R_2$, $R_c = R/2$. The work of adhesion E_{ad} can be calculated using the following equation for two flat surfaces separated by a distance D (Israelachvili 1992):

$$E_{ad} = -\frac{H}{12\pi D^2}, \tag{2.12}$$

where H is the Hamakar constant that depends on the medium the two surfaces are in. Typical values of the Hamakar constant for polymers are $H_{air} = 10^{-19}$ J in the air and $H_{water} = 3.7\times10^{-20}$ J in the water (Israelachvili 1992). The work of adhesion of two surfaces in contact separated by an atomic distance $D \approx 0.2$ nm (Israelachvili 1992) is approximately equal to -66 mJ m^{-2} in the air and -44 mJ m^{-2} in the water. Assuming tip radius R is 50 nm, the DMT adhesion forces of a single contact in the air and the water are $F_{DMT}^{air} = 11$ nN and $F_{DMT}^{water} = 7.3$ nN, respectively. As the humidity increases from 0 to 100%, the DMT adhesion force will take a value between F_{DMT}^{air} and F_{DMT}^{water}. To calculate the DMT adhesion force for the intermediate humidity, an approximation method by Wan *et al.* (1992) is used. The work of adhesion E_{ad} for the intermediate humidity can be expressed as

$$E_{ad} = \int_D^\infty \frac{H}{6\pi h^3}\,dh = \int_D^{h_f} \frac{H_{water}}{6\pi h^3}\,dh + \int_{h_f}^\infty \frac{H_{air}}{6\pi h^3}\,dh, \tag{2.13}$$

where h is the separation along the plane. h_f is the water film thickness at a filling angle ϕ, which can be calculated as

$$h_f = D + R(1-\cos\phi). \tag{2.14}$$

Note that Wan *et al.*'s model has a limitation that the H_{air} in equation (2.13) may not be suitable since there will be always liquid contact between the tip and water layer. As discussed by Israelachvili (1992), when there is a water layer in between two solids, the Hamakar constant would be almost 10 times smaller, and van der Waals force values decrease.

Using equations (2.11), (2.13) and (2.14), the DMT adhesion force for the intermediate humidity is given as

$$F_{DMT} = F_{DMT}^{water}\left\{1 - \frac{1}{(1+R(1-\cos\phi)/D)^2}\right\} + F_{DMT}^{air}\left\{\frac{1}{(1+R(1-\cos\phi)/D)^2}\right\}. \tag{2.15}$$

Finally, total adhesion force is calculated as the sum of equations (2.10) and (2.15)

$$F_{\mathrm{ad}} = F_{\mathrm{c}} + F_{\mathrm{DMT}}. \tag{2.16}$$

Total adhesion force is used as a critical force in the spring model. In the spring model for gecko seta, if the force applied upon spring deformation is greater than the adhesion force, the spring is regarded as having been detached.

2.2. Simplification in the hierarchical morphology of setae

The seta manifests a hierarchical structure—thicker parts branched into thinner ones. In this study, we focus on the *T. gecko*—the most extensively studied species. The attachment pads of *T. gecko* feet consist of an intricate hierarchy of structures beginning with lamellae, soft ridges that are approximately 1–2 mm in length, located on the attachment pads (toes) as shown schematically in figure 2*a*. Tiny curved hairs known as setae extend from the lamellae. These setae are typically 30–130 μm in length and 5–10 μm in diameter. The setae of a gecko have several branches. Each seta branches into several hundred substructures (Ruibal & Ernst 1965; Hiller 1968; Russell 1975; Williams & Peterson 1982) called spatulae. A branched seta looks like a broom and has a length of approximately 20–30 μm and a diameter of approximately 1–2 μm (Ruibal & Ernst 1965). The tips of the spatulae have a typical size of the order of 500 nm in length, 200–300 nm in width and approximately 10 nm in thickness (Ruibal & Ernst 1965; Williams & Peterson 1982; Persson & Gorb 2003). Spatulae are oriented at an angle with respect to the contacting surface to facilitate peeling. Setae are composed of β-keratin with an elastic modulus in the range 1–20 GPa (Russell 1986; Bertram & Gosline 1987).

We approximate a gecko seta with a hierarchical spring model (figure 2*b*). Each level of springs in the model corresponds to a level of seta hierarchy. The upper level of springs corresponds to the thicker part of gecko seta, the middle part to the branches and the lower part to the spatulae. The upper level is the thickest branch of a seta. It is 75 μm in length and 5 μm in diameter. The middle level, referred to as branch, has a length of 25 μm and diameter of 1 μm. The lower level, called a spatula, is the thinnest branch with a length of 2.5 μm and a diameter of approximately 0.1 μm. Autumn *et al.* (2000) showed that the optimal attachment angle, φ, between the substrate and a gecko seta is 30° in the single seta pull-off experiment. This finding is supported by the adhesion models of setae as cantilever beams (Sitti & Fearing 2003; Gao *et al.* 2005). Therefore, in this study, φ is fixed at 30°.

2.3. The multi-level hierarchical spring analysis

The adhesion simulation of three-level hierarchy for gecko seta in contact with random surface is carried out numerically. The springs on every level of hierarchy have the same stiffness as the bending stiffness of the corresponding branches of seta. If the beam is oriented at an angle φ to the substrate and the contact load F is aligned normal to the substrate, the stiffness of seta branches k_m is calculated as (Young & Budynas 2001)

$$k_m = \frac{\pi R_m^2 E}{l_m \sin^2\theta\left[1 + \frac{4l_m^2 \cot^2\varphi}{3R_m^2}\right]}, \tag{2.17}$$

where l_m and R_m are the length and the radius of seta branches, respectively, and m is the level number. The three-level model considered here has springs with length $l_{\mathrm{I}}=2.5$ μm, $l_{\mathrm{II}}=25$ μm and $l_{\mathrm{III}}=75$ μm for levels I, II and III, respectively. For an assumed elastic modulus E of seta material of 10 GPa with a load applied at an angle of 60° to spatulae long axis, the stiffness of every level of seta is calculated as $k_{\mathrm{I}}=0.0126$ N m^{-1}, $k_{\mathrm{II}}=0.126$ N m^{-1} and $k_{\mathrm{III}}=2.908$ N m^{-1}, respectively.

The base of the springs and the connecting plate between the levels are assumed to be rigid. The distance s_{I} between neighbouring structures of level I is 0.35 μm, obtained from the average value of measured spatula density, 8×10^6 mm^{-2}, obtained by multiplying 14 000 setae mm^{-2} by an average of 550 spatulae per seta (Schleich & Kästle 1986). Assuming a 1 : 10 proportion of the number of springs in the upper level to that in the lower level, one spring at level III is connected to 10 springs on level II and each spring on level II also has 10 springs on level I. The number of springs, N_{I}, considered here is calculated by dividing the scan length (2000 μm selected here) with the distance s_{I} (0.35 μm) and corresponds to 5700.

The deflection of spring Δl was calculated as

$$\Delta l = h - l_0 - z, \tag{2.18}$$

where h is the position of the spring base relative to the mean line of surface; l_0 is the total length of a spring structure which is $l_0 = l_{\mathrm{I}} + l_{\mathrm{II}} + l_{\mathrm{III}}$; and z is the profile height of the rough surface. The elastic force F_{el} arisen in the springs at a distance h from the surface was calculated for the three-level model as

$$F_{\mathrm{el}} = -\sum_{k=1}^{r}\sum_{j=1}^{q}\sum_{i=1}^{p} k_{kji}(\Delta l_{kji} - \Delta l_{kj} - \Delta l_k)u_{kji}$$

$$u_{kji} = \begin{cases} 1 & \text{if contact} \\ 0 & \text{if no contact} \end{cases}, \tag{2.19}$$

where p, q and r are the number of springs in the levels I, II and III of the model, respectively. When springs approach the rough surface, the spring force is calculated using equation (2.19). During pull-off, the same equations are used to calculate the spring force. However, when the applied load is equal to zero, the springs do not detach due to adhesion attraction given by equation (2.16). Springs are pulled apart until the net force (pull-off force minus attractive adhesion force) at the interface is equal to zero. The adhesion force is the lowest value of elastic force F_{el} when the seta has detached from the contacting surface.

The random rough surfaces used for simulation were generated by a computer program (Bhushan 1999, 2002). The roughness parameters are scale dependent and, therefore, adhesion values also are expected to be scale dependent. Increase in the scan length led to increase in both RMS amplitude and correlation length

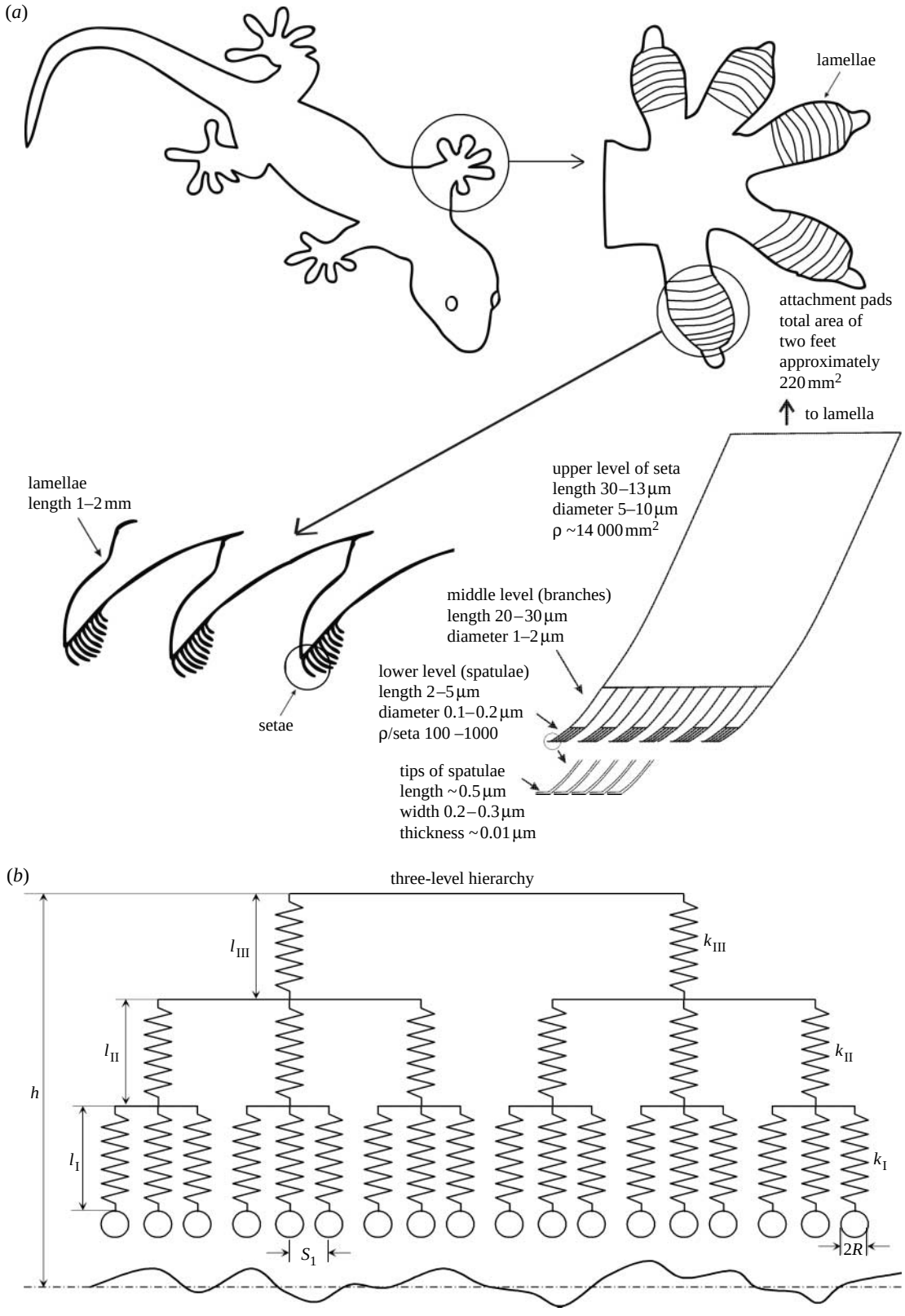

Figure 2. (*a*) Schematic drawings of a *T. gecko* including the overall body, one foot, a cross-sectional view of the lamellae and an individual seta with three levels of branches: seta level; middle level; and spatula level. ρ shown in the figure is the seta density per unit area. (*b*) Three-level spring models for the simulation effect of hierarchical morphology on the interaction of a seta with a rough surface. In this figure, l_I, l_{II} and l_{III} are lengths of structures; s_I is space between spatulae; k_I, k_{II} and k_{III} are stiffnesses of structures; I, II and III are level indexes; R is the radius of tip; and h is the distance between upper spring base of each model and mean line of the rough profile.

(Bhushan *et al.* 2006). For the modelling of contact of attachment system with random rough surfaces, the range of values of σ from 0.01 to 10 μm and a fixed value of $\beta^* = 200$ μm were taken. The chosen range covers values of roughnesses for relatively smooth artificial surfaces to natural rough surfaces. A typical scan length of 2000 μm was also chosen, which is comparable to a lamella length of a gecko.

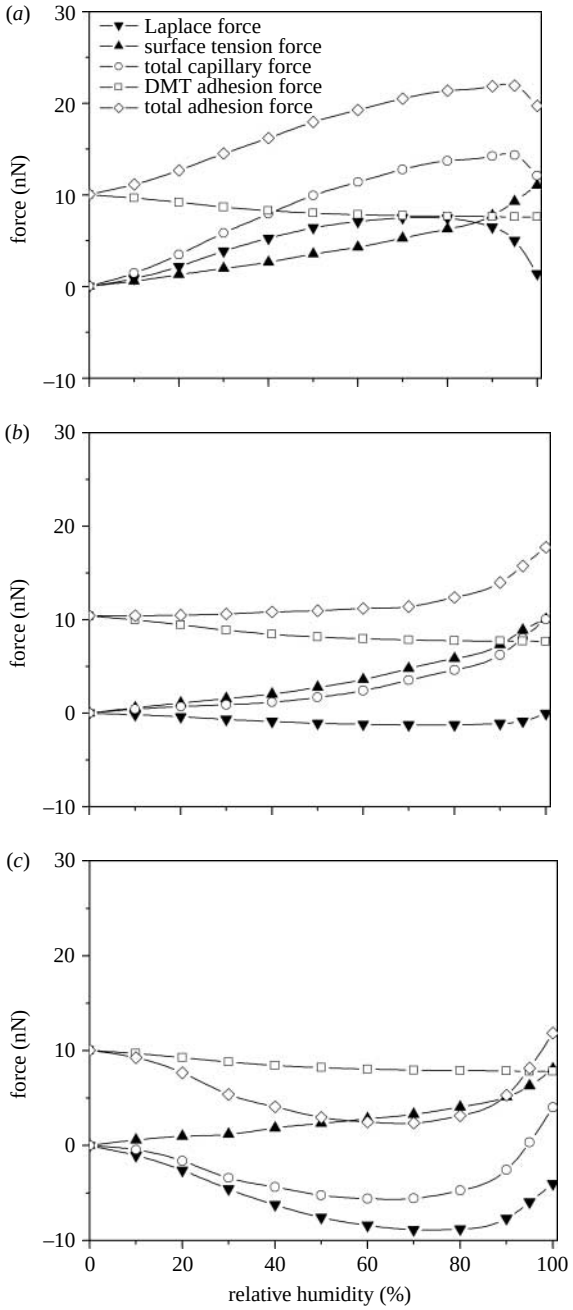

Figure 3. The variation of the Laplace force, the surface tension force, total capillary force, the DMT adhesion force and total adhesion force with relative humidity for three different contact angles of substrate. $R=50$ nm, $\gamma=73$ mJ m^{-2}, $V=0.03$ nm^3, $\theta_1=128°$. (*a*) $\theta_2=10°$, (*b*) $\theta_2=58°$ and (*c*) $\theta_2=110°$.

3. RESULTS AND DISCUSSION

In order to investigate the effects of capillarity on gecko adhesion, we considered the capillary force consisting of the Laplace force and the surface tension force as well as the solid-to-solid interaction by DMT theory. First, the adhesion forces exerted by a single gecko spatula in contact with planes with different contact angles for various relative humidity are calculated and compared with experimental data. Next, we performed the adhesion analysis for three-level hierarchical model for gecko seta in contact with rough surfaces with different σ values.

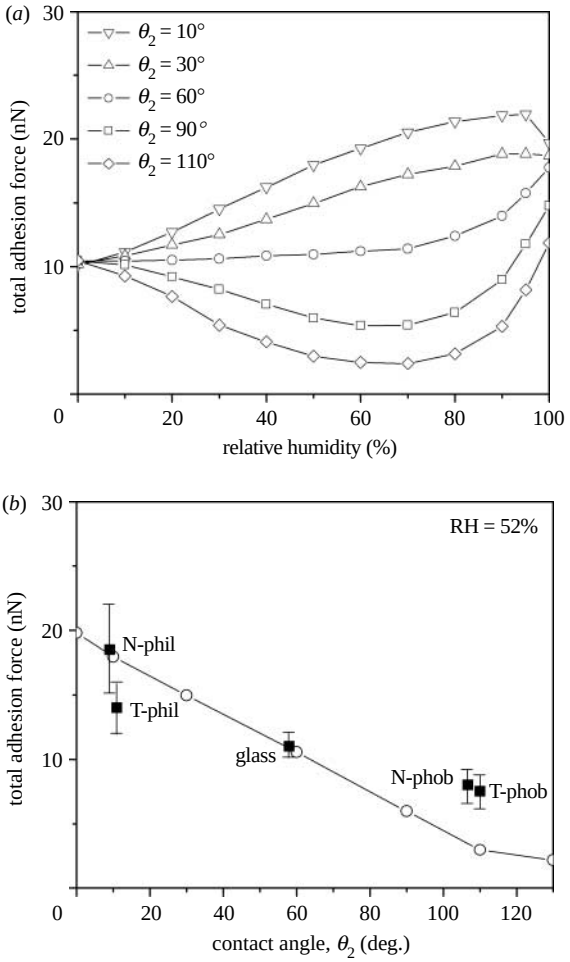

Figure 4. (*a*) Total adhesion force as a function of relative humidity for a single spatula in contact with surfaces with different contact angles. (*b*) Comparison of the simulation results with the measured data for a single spatula in contact with the hydrophilic and the hydrophobic surfaces (Huber *et al.* 2005). $R=50$ nm, $\gamma=73$ mJ m^{-2}, $V=0.03$ nm^3, $\theta_1=128°$.

To simulate the capillarity contributions to adhesion force for gecko spatula, the contact angle on gecko spatula tip θ_1 is set as a value of 128° in the subsequent analysis (Huber *et al.* 2005). It is assumed that the spatula tip radius $R=50$ nm, the ambient temperature $T=25°$C, the surface tension $\gamma=73$ mJ m^{-2} and molecular volume of water $V=0.03$ nm^3 (Israelachvili 1992). At a given environment, we can calculate the filling angle ϕ by equations (2.3) and (2.4). Then, capillary force together with the contribution of the Laplace force and the surface tension force can be calculated using equation (2.10).

Figure 3 shows the variation of the capillary force, the DMT adhesion force and total adhesion force with relative humidity for three different contact angles of the substrate. The contact angles $\theta_2=10°$ and 110° used here correspond to hydrophilic Si wafer- and hydrophobic Si wafer-covered octadecyltrichlorosilane, respectively (Huber *et al.* 2005). For the hydrophilic surface of $\theta_2=10°$, the Laplace force increases to a somewhat saturated value at intermediate humidity, and then decreases rapidly at a value of the relative humidity of more than 80%. The contribution of the

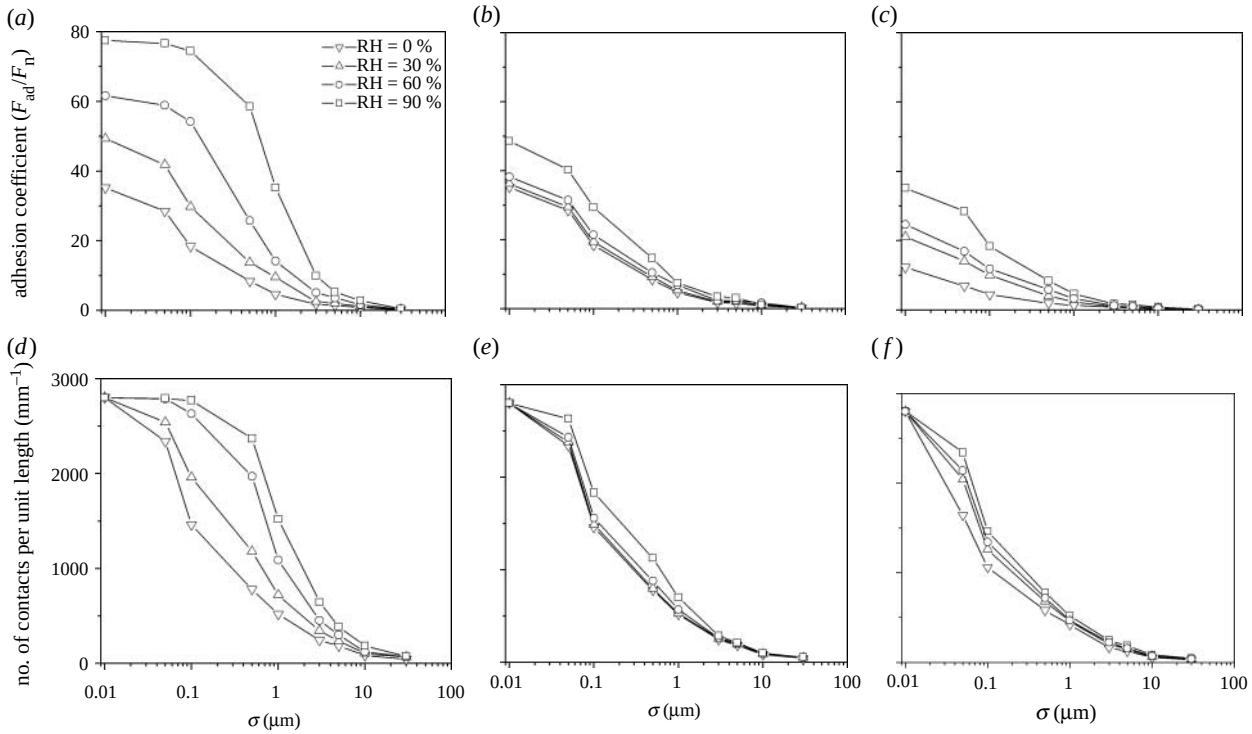

Figure 5. The adhesion coefficient and the number of contacts per unit length for three-level hierarchical model in contact with rough surfaces with different values of RMS amplitude σ and contact angles for different relative humidity. $F_n=1.6$ μN, $\beta=200$ μm, $R=50$ nm, $\gamma=73$ mJ m^{-2}, $V=0.03$ nm^3, $\theta_1=128°$. (*a*,*d*) $\theta_2=10°$, (*b*,*e*) $\theta_2=58°$ and (*c*,*f*) $\theta_2=110°$.

surface tension increases slowly, but rises rapidly at a value of the relative humidity of more than 80%. The total capillary force increases to 22 nN at 95% relative humidity and decreases at the higher relative humidity. Owing to the mutual compensation of the contributions of the Laplace force and the surface tension force, the decrease of total capillary force is not drastic. The DMT adhesion force decreases with an increase in relative humidity. The contribution of the DMT adhesion force occupies a large portion in total adhesion force.

The surface tension force and the DMT adhesion force for the surface of $\theta_2=58°$ are similar to those for the surface of $\theta_2=10°$, but the Laplace force, contrary to the case of $\theta_2=10°$, has slightly negative values through all the relative humidity. It is shown that surface tension force occupies a larger portion in the capillary force in this case. Total adhesion force increases slowly to 12 nN at a value of relative humidity of 80% and rapidly at the higher relative humidity due to the compensation of the capillary force and the DMT adhesion force. The Laplace force for the hydrophobic surface of $\theta_2=110°$ decreases at the values of the relative humidity less than 80% with negative values and then increases. Owing to the larger contribution of the Laplace force, both the capillary and total adhesion forces have a similar tendency with the Laplace force.

From figure 3, it is shown that the Laplace force as well as the DMT adhesion force gives the larger effect on total adhesion force. For a given spatula tip that is a hydrophobic surface, as the contact angle of the substrate increases, a mean curvature of meniscus formed between two surfaces changes from negative to positive values and the pressure inside the meniscus becomes higher than outside, which results in a decrease of capillary force.

Figure 4*a* shows the total adhesion force as a function of relative humidity for a single spatula in contact with surfaces with different contact angles. Total adhesion force decreases with an increase in the contact angle on the substrate, and the difference of total adhesion force among contact angles is larger in the intermediate humidity regime. As the relative humidity increases, total adhesion force for the surfaces with contact angle less than 60° has a higher value than the DMT adhesion force not considering wet contact, whereas above a value of 60°, total adhesion force has lower values at most relative humidities. The simulation results of this analysis are compared with the experiment data by Huber *et al.* (2005) in figure 4*b*. They measured the pull-off force of a single spatula in contact with four different types of Si wafer and glass at the ambient temperature 25°C and the relative humidity 52%. According to their description, wafer families 'N' and 'T' in figure 4*b* differ by the thickness of the top amorphous Si oxide layer. The 'Phil' type is cleaned Si oxide surfaces, which is hydrophilic with a water contact angle of approximately 10°, whereas the 'Phob' type is Si wafer-covered hydrophobic monolayer causing water contact angle to be greater than 100°. The glass has water contact angle of 58°. They showed that the adhesion force of a gecko spatula rises significantly for substrates with increasing hydrophilicity. In figure 4*b*, the simulation results are in good agreement with their experimental results.

We performed the adhesion analysis for three-level hierarchical model for gecko seta. Figure 5 shows the adhesion coefficient and number of contacts per unit length for three-level hierarchical models in contact with rough surfaces with different values of RMS amplitude σ ranging from 0.01 to 30 μm for different

relative humidity and contact angles of surface. The applied load of 1.6 μN used here is derived from the gecko's weight (Kim & Bhushan 2007). Adhesion coefficient is the ratio of applied preload to pull-off force, which represents the strength of adhesion as a function of the preload. For the surface with contact angle $\theta_2 = 10°$ and relative humidity of 0%, the maximum adhesion coefficient is approximately 36 at value of σ smaller than 0.01 μm. It means gecko feet can generate enough adhesion force to support 36 times the gecko's weight. However, the adhesion coefficient decreases with an increase in σ value. By increasing σ up to 1 μm, the adhesion coefficient is reduced rapidly to approximately 5, and then for the surface with σ more than 10 μm decreases to a value less than 1, which cannot support the gecko weight. It is shown that the trends in the number of contacts are similar to that of the adhesion force. Here, the number of contacts means the number of springs in level I when the maximum adhesion force occurs. For the surface with contact angle of $\theta_2 = 10°$, the adhesion coefficient increases with an increase of relative humidity: the adhesion coefficient for relative humidity of 90% has two times higher value than that for relative humidity of 0% at a value of σ smaller than 0.01 μm. Even on the surface with σ of 10 μm, the adhesion force is more than three times the gecko weight. However, the adhesion enhancement by the increase of relative humidity is reduced in the surface with larger contact angle. In the surface with contact angle of $\theta_2 = 58°$, a little increment of the adhesion coefficient is observed, and in the surface with contact angle of $\theta_2 = 110°$; on the contrary, the adhesion coefficient significantly decreases with an increase of the relative humidity. Therefore, we can say that hydrophilic surface is beneficial to gecko adhesion enhancement.

4. CONCLUSIONS

In this study, we investigated the effects of capillarity on gecko adhesion. We considered the capillary force consisting of the Laplace force and the surface tension force as well as the DMT adhesion force.

The adhesion forces exerted by a single gecko spatula in contact with planes with different contact angles for various relative humidity are calculated. The surface tension force always decreases with increase in relative humidity regardless of the hydrophobicity of the surface, whereas the Laplace force shows different behaviour according to hydrophilic or hydrophobic surface. The Laplace force for the hydrophilic surface increases at intermediate humidity and then decreases rapidly at a value of relative humidity more than 80%, but for the hydrophobic surface, decreases at values of relative humidity less than 80% with negative values and then increases. The DMT adhesion force decreases with an increase in relative humidity. The contribution of the DMT adhesion force occupies a large portion in total adhesion force and the capillary force is comparable with DMT force. Total adhesion force decreases with an increase in the contact angle on the substrate, and the difference of total adhesion force among contact angles is larger in the intermediate humidity regime. In addition, we showed that the simulation results are in good agreement with the experimental results for a single spatula in contact with the hydrophilic and the hydrophobic surfaces.

The adhesion analysis for three-level hierarchical model for gecko seta in contact with rough surfaces with different σ values has been carried out. It is shown that hydrophilic surface is beneficial to gecko adhesion enhancement. For the surface with contact angle of $\theta_2 = 10°$, the adhesion coefficient increases with an increase of relative humidity. However, the adhesion enhancement by an increase of the relative humidity decreases in the surface with larger contact angle.

REFERENCES

Arzt, E., Gorb, S. & Spolenak, R. 2003 From micro to nano contacts in biological attachment devices. *Proc. Natl Acad. Sci. USA* **100**, 10 603–10 606. (doi:10.1073/pnas.1534701100)

Autumn, K., Liang, Y. A., Hsieh, S. T., Zesch, W., Chan, W. P., Kenny, T. W., Fearing, R. & Full, R. J. 2000 Adhesive force of a single gecko foot-hair. *Nature* **405**, 681–685. (doi:10.1038/35015073)

Autumn, K. *et al.* 2002 Evidence of van der Waals adhesion in gecko setae. *Proc. Natl Acad. Sci. USA* **99**, 12 252–12 256. (doi:10.1073/pnas.192252799)

Bergmann, P. J. & Irschick, D. J. 2005 Effects of temperature on maximum clinging ability in a diurnal gecko: evidence for a passive clinging mechanism? *J. Exp. Zool. A* **303**, 785–791. (doi:10.1002/jez.a.210)

Bertram, J. E. A. & Gosline, J. M. 1987 Functional design of horse hoof keratin: the modulation of mechanical properties through hydration effects. *J. Exp. Biol.* **130**, 121–136.

Bhushan, B. 1999 *Principles and applications of tribology.* New York, NY: Wiley.

Bhushan, B. 2002 *Introduction to tribology.* New York, NY: Wiley.

Bhushan, B. 2003 Adhesion and stiction: mechanisms, measurement techniques, and methods for reduction. *J. Vac. Sci. Tech. B* **21**, 2262–2296. (doi:10.1116/1.1627336)

Bhushan, B., Peressadko, A. G. & Kim, T. W. 2006 Adhesion analysis of two-level hierarchical morphology in natural attachment systems for 'smart' adhesion. *J. Adhes. Sci. Technol.* **20**, 1475–1491. (doi:10.1163/156856106778666408)

Carter, W. C. 1988 The force and behavior of fluids constrained by solids. *Acta Metall.* **36**, 2283–2292. (doi:10.1016/0001-6160(88)90328-8)

Derjaguin, B. V., Muller, V. M. & Toporov, Yu. P. 1975 Effect of contact deformation on the adhesion of particles. *J. Coll. Interface Sci.* **53**, 314–326. (doi:10.1016/0021-9797(75)90018-1)

Fortes, M. A. 1982 Axisymmetric liquid bridges between parallel plates. *J. Coll. Interface Sci.* **88**, 338–352. (doi:10.1016/0021-9797(82)90263-6)

Gao, H., Wong, X., Yao, H., Gorb, S. & Arzt, E. 2005 Mechanics of hierarchical adhesion structures of geckos. *Mech. Mater.* **37**, 275–285. (doi:10.1016/j.mechmat.2004.03.008)

Hiller, U. 1968 Untersuchungen zum feinbau und zur funktion der haftborsten von reptilien. *Z. Morph. Tiere* **62**, 307–362. (doi:10.1007/BF00401561)

Huber, G., Mantz, H., Spolenak, R., Mecke, K., Jacobs, K., Gorb, S. N. & Arzt, E. 2005 Evidence for capillarity contributions to gecko adhesion from single spatula and nanomechanical measurements. *Proc. Natl Acad. Sci. USA* **102**, 16 293–16 296. (doi:10.1073/pnas.0506328102)

Irschick, D. J., Austin, C. C., Petren, K., Fisher, R. N., Losos, J. B. & Ellers, O. 1996 A comparative analysis of clinging

ability among pad-bearing lizards. *Biol. J. Linn. Soc.* **59**, 21–35. (doi:10.1006/bijl.1996.0052)

Israelachvili, J. N. 1992 *Intermolecular and surface forces*. San Diego, CA: Academic Press.

Jagota, A. & Bennison, S. J. 2002 Mechanics of adhesion through a fibrillar microstructure. *Integr. Comp. Biol.* **42**, 140–1145. (doi:10.1093/icb/42.6.1140)

Johnson, K. L., Kendall, K. & Roberts, A. D. 1971 Surface energy and the contact of elastic solids. *Proc. R. Soc. A* **324**, 301–313. (doi:10.1098/rspa.1971.0141)

Kim, T. W. & Bhushan, B. 2007 Adhesion analysis of multi-level hierarchical attachment system contacting with rough surface. *J. Adhes. Sci. Technol.* **21**, 1–20. (doi:10.1163/156856107779976097)

Kim, T. W. & Bhushan, B. In press. Effect of stiffness of multi-level hierarchical attachment system on adhesion enhancement, *Ultramicroscopy*.

Northen, M. T. & Turner, K. L. 2005 A batch fabricated biomimetic dry adhesive. *Nanotechnology* **16**, 1159–1166. (doi:10.1088/0957-4484/16/8/030)

Orr, F. M., Scriven, L. E. & Rivas, A. P. 1975 Pendular rings between solids: meniscus properties and capillary force. *J. Fluid Mech.* **67**, 723–742. (doi:10.1017/S0022112075000572)

Persson, B. N. J. & Gorb, S. 2003 The effect of surface roughness on the adhesion of elastic plates with application to biological systems. *J. Chem. Phys.* **119**, 11 437–11 444. (doi:10.1063/1.1621854)

Ruibal, R. & Ernst, V. 1965 The structure of the digital setae of lizards. *J. Morphol.* **117**, 271–293. (doi:10.1002/jmor.1051170302)

Russell, A. 1975 A contribution to the functional analysis of the foot of the *Tokay*, *Gekko gecko* (Reptilia: Gekkonidae). *J. Zool. Lond.* **176**, 237–476.

Russell, A. 1986 The morphological basis of weight-bearing in the scansors of the *Tokay gecko*. *Can. J. Zool.* **64**, 948–955.

Schleich, H. H. & Kästle, W. 1986 Ultrastrukturen an Gecko-Zehen. *Amphibia-Reptilia* **7**, 141–166.

Sitti, M. 2003 High aspect ratio polymer micro/nano-structure manufacturing using nanoembossing, nano-molding and directed self-assembly. In *Proc. IEEE/ASME Advanced Mechatronics Conf., 20–24 July*, 2, pp. 886–890.

Sitti, M. & Fearing, R. S. 2003 Synthetic gecko foot-hair micro/nano-structures as dry adhesives. *J. Adhes. Sci. Technol.* **17**, 1055–1073. (doi:10.1163/156856103322113788)

Stifter, T., Marti, O. & Bhushan, B. 2000 Theoretical investigation of the distance dependence of capillary and van der Waals forces in scanning force microscopy. *Phys. Rev. B* **62**, 13 667–13 673. (doi:10.1103/PhysRevB.62.13667)

Wan, K. T., Smith, D. T. & Lawn, B. R. 1992 Fracture and contact adhesion energies of mica–mica, silica–silica, and mica–silica interfaces in dry and moist atmospheres. *J. Am. Ceram. Soc.* **75**, 667–676. (doi:10.1111/j.1151-2916.1992.tb07857.x)

Williams, E. E. & Peterson, J. A. 1982 Convergent and alternative designs in the digital adhesive pads of scincid lizards. *Science* **215**, 1509–1511. (doi:10.1126/science.215.4539.1509)

Young, W. C. & Budynas, R. 2001 *Roark's formulas for stress and strain*, 7th edn. New York, NY: McGraw Hill.